Computer Aided Design and Optimization of Integrated Circuits with RF MEMS Devices by an ANN Based Macro-Modeling Approach

Yongjae Lee[*], Yonghwa Park[**], Feng Niu[***], and Dejan S. Filpovic[*]

[*]University of Colorado, Boulder, CO, USA, {yongjae, dejan}@colorado.edu
[**] Samsung Electronics, Co., Ltd., Suwon, Korea, yongh.park@samsung.com
[***]Motorola, Inc., Plantation, FL, USA, F.niu@motorola.com

ABSTRACT

Artificial neural network (ANN) based macro-modeling approach for design and optimization of integrated circuits (ICs) with radio frequency microelectromechanical systems (RF MEMS) is presented. The finite element method (FEM) analysis is utilized for both characterization of the device and generation of training and testing data for the ANN model. Developed ANN based approach has shown excellent agreement with the FEM model and measurements. The integration of the ANN model in an RF circuit simulator shows that the proposed methodology is suitable for a circuit-level analysis, design, and optimization of MEMS devices.

Keywords: artificial neural network, backpropagation, computer aided design, finite element methods, microelectromechanical devices.

1 INTRODUCTION

As the complexity of RF MEMS devices and their usage in modern ICs and RF applications is increased, more accurate and efficient computer aided design (CAD) tools are required. The main objective is to reduce time and cost in a design process which traditionally has relied on experiments. Currently proposed full-wave techniques for RF MEMS devices include the FEM [1-3] and finite difference time domain (FDTD) [4]. These techniques usually show good accuracy. However, large memory requirement and inability for effective modeling on the system level limit their use for primarily individual device-level analysis. To realize a circuit-level simulation, lumped circuit model [5] and macromodeling approaches [6-7] are proposed. These approaches provide large reductions in simulation time while preserving adequate accuracy. However, the design and optimization of the electronics incorporating MEMS devices are still problematic. To alleviate above mentioned limitations, we utilize the ANN technique for modeling, design and optimization of MEMS devices at the device, circuit and/or system levels. Although ANNs require extensive time and effort for preparing a training set, once the network is trained, it enables efficient correlation between unknown physical input and corresponding output responses within the range of training data. Figure 1 shows the algorithm of the proposed methodology. Note that a similar scheme is reported in our earlier work [8].

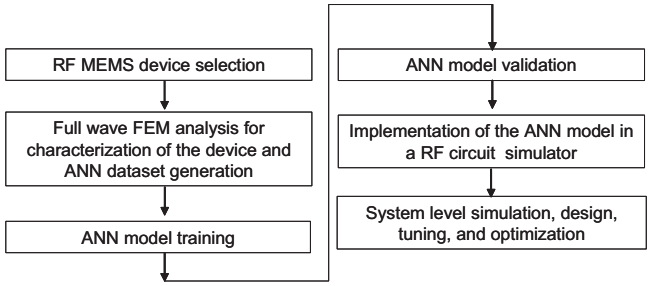

Figure 1: Schematic of ANN based macromodeling approach

In this paper, a Free-Free (FF) beam MEMS resonating structure [9] is chosen for demonstration. An in-house FEM solver [10] is utilized for characterization of the resonator's electromechanical behavior and generation of input and output datasets. Several ANN architectures are studied and backpropagation with Levenberg-Marquardt algorithm is selected. Once the training is completed, the ANN blackbox models of the resonator are integrated within a 30MHz Pierce oscillator and simulated in Advanced Design System (ADS) circuit simulator environment [11]. Then, optimization of the device and a circuit as a whole is performed in ADS. Excellent agreement between the optimized ANNs and FEM simulations validates proposed approach. For a single geometry simulation, direct comparison between FEM and ANN analysis amounts to approximately 30 times reduction in running time with ANNs.

This paper is organized as follows: in Section 2, a description of the FEM analysis is given. ANN modeling procedure is presented in Section 3. Implementation, simulation, and optimization with ANNs in a circuit simulator are discussed in Section 4.

2 FINITE ELEMENT MODELING OF A FREE-FREE BEAM RF MEMS RESONATOR

A schematic of a FF beam MEMS resonator [9] is shown in Figure 2. The resonator consists of a resonating beam supported at its flexural node points (L_{n1} and L_{n2}) by four flexural beams fixed to the substrate by rigid contact anchors.

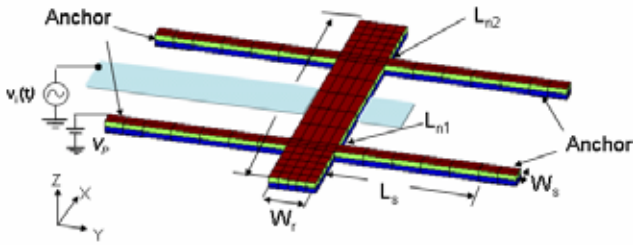

Figure 2: FEM model of a FF beam RF MEMS resonator.

Parameter	Target frequency		Unit
	~50	~90	MHz
R. beam length, L_r	17.8	13.1	µm
R. beam width, W_r	10	6	µm
Supporting beam length, L_s	18.4	10.3	µm
Supporting beam width, W_s	1	1	µm
Node location 1, L_{n1}	4	2.9	µm
Node location 2, L_{n2}	13.8	10.2	µm
Electrode width, *We*	4.5	2.8	µm
Initial gap, *d*	1230	1230	Å
DC bias voltage, V_p	86	76	V
Young's modulus	150		Gpa
Poisson's ratio	0.226		–
AC excitation	5		mV

Table 1: Material properties used in FEM simulation of a FF beam RF MEMS resonator [9].

The AC excitation and DC bias voltage are applied across the electrode and resonating beam, generating the time-varying capacitance between the beam and the underlying electrode. The modal superposition technique [12] based FE solver is utilized to capture the dynamic characteristics including electro-mechanical coupling effects. Detailed geometries and material properties used for the simulation are shown in Table 1. The resonator's transfer function, defined as the ratio of the output current and AC driving voltage, is computed for 100 electromechanical modes. Figure 3 shows the modal analysis results for ~50 and ~90MHz resonators. The accuracy of the FE prediction is assessed via the comparisons with the measurements [9]. Relative errors for the resonant frequencies of the dominant modes for ~50MHz and ~90MHz are 2.4% and 1.7%, respectively. This discrepancy is likely due to the slight difference in the structural parameters (the depletion region, depth of dimples, etching depth of sacrificial layer, etc.) between the fabricated device and that used in the numerical model. The eigenvectors for the dominant modes (mode shapes) are extracted based on the computation of the largest deflection at the center of the resonating beam. First two dominants modes are of interest for this work. Physically, these modes have vertical deformations of the resonating beam so that they can be easily excited at the center of the beam.

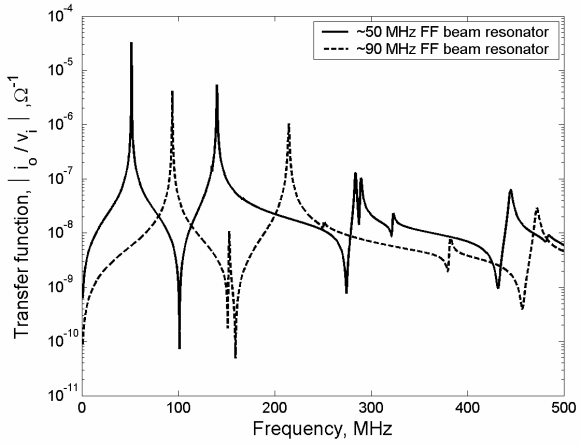

Figure 3: FEM solver computed transfer function for the target frequencies of ~50MHz and ~90MHz FF beam MEMS resonators.

3 ANN MODELING

For the RF/microwave modeling and design, a multilayer feed-forward network has been traditionally utilized [13]. The performance of ANNs is evaluated by computing the difference between outputs from ANNs and training datasets. This term is often called *Correlation coefficient* (R^2),

$$R^2 = 1 - \frac{\sum_{m=1}^{S}\sum_{l=1}^{n}(y_{ml}(\omega) - \hat{y}_{ml})^2}{\sum_{m=1}^{S}\sum_{l=1}^{n}(y_{ml}(\omega) - \bar{y}_{ml})^2} \quad (1)$$

where S is the number of training datasets, n is the number of samplings in output variables, $[\hat{y}_{ml}]$ and $[y_{ml}]$ are outputs from the FEM and the ANN model, respectively, and $\bar{y}_{ml}$ is the mean of the ANN model.

To determine the number of neurons and hidden layers, a number of simulations are performed by varying numbers of neurons and hidden layers. The number of neurons in the hidden layer is critical to the generalization of ANN models. Too many neurons in the hidden layer often contribute to *overfitting*, while a network with too few neurons may not be able to learn the desired input/output mapping. R^2 is monitored for the cases with one and two hidden layers (see Figure 4). As a result, the higher correlation coefficient is observed with two hidden layers than with one hidden layer. For both cases, overlearning begins at the point where the correlation coefficient starts decreasing after reaching the maximum point.

Based on these results, a feed-forward backpropagation network with two hidden layers (with 8 neurons in each layer) is developed. The Levenberg Marquardt algorithm is used for training ANNs. A total of 150 training datasets and 60 testing datasets are generated using composite design technique [14]. The feasible range of input variables is given in Table 2.

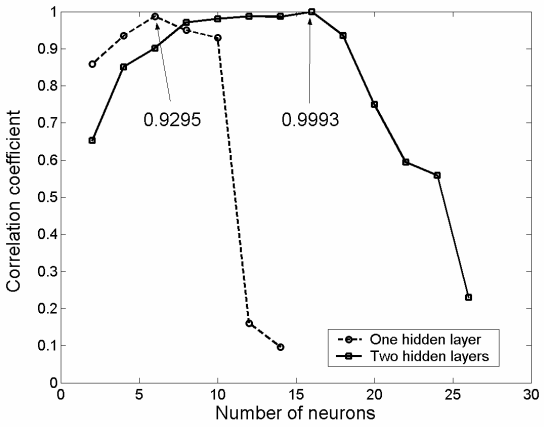

Figure 4: Correlation coefficient between the ANN model and testing datasets.

Input variables	Range	Increment	Unit
Resonator beam length	10~33	2.5	μm
Gap	0.08~0.16	0.04	μm
DC bias	10~150	30	V

Table 2: The range for the ANN input variables.

1st mode target frequency	FEM model [MHz]	ANN model [MHz]	Relative error	Measure-ment [MHz]
~30MHz	31.09	31.06	0.10%	31.51
~50MHz	51.56	51.53	0.06%	50.35
~70MHz	72.56	72.42	0.20%	71.49
~90MHz	93.85	94.17	0.30%	92.25

Table 3: Comparisons between ANN model, FEM model and measurements [9].

Table 3 shows the validation of the developed ANN model with the FE simulations and measurements. Note that the relative errors less than 0.5% are computed with respect to the FEM model.

4 ANN MODEL INTEGRATION AND CIRCUIT LEVEL OPTIMIZATION

To demonstrate additional capability of the proposed approach, the ANN blackbox model of the FF beam resonator is integrated in a 30MHz Pierce oscillator (see Figure 5). Optimized weight and bias matrices are implemented within a framework of ADS circuit simulator. As seen, the circuit implementation of the ANN model offers great advantages for overall complex circuit simulation. Specifically, the performance of the RF MEMS resonator within an IC circuit is optimized in a circuit simulator. Optimized values can then be used as a guideline for the design of ICs incorporating the very same resonator.

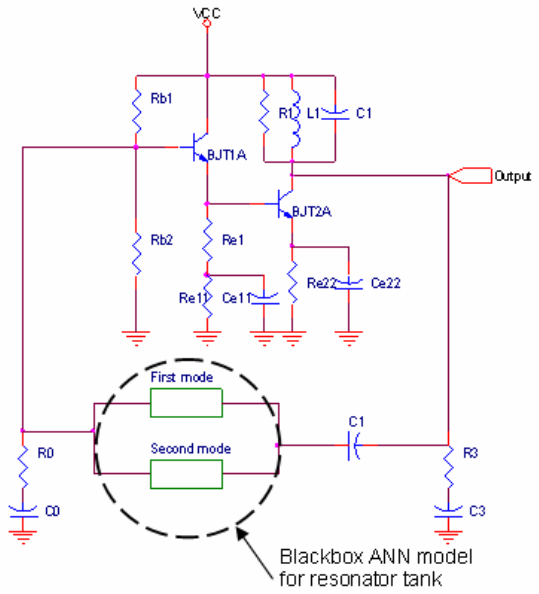

Figure 5: Schematic of the modified Pierce oscillator with the implemented ANN model.

Parameters	Values	Parameters	Values
Vcc	4 V	C1	1.38fF
Rb1	600kΩ	Re22	1kΩ
Rb2	2475kΩ	Ce22	0.1μF
Re1	15kΩ	R0	5Ω
Re11	3kΩ	R3	10Ω
Ce11	0.1μF	C0	4.7pF
R1	1MΩ	C3	0.9pF
L1	270μH		

Table 4: Values for the Pierce oscillator circuit components.

As an example, given is the goal to design a 30MHz oscillator with ultra-low phase noise. The initial values for the structural parameters of the resonator are:

- Length of the resonator (L_r=23.2μm)
- Gap between the resonating beam and the electrode (d=1230Å)
- DC bias voltage (V_p=22V)

After 361secs and 25 iterations using gradient method, the optimized values of structural parameters are:

- L_r = 23.56μm (1.6% increase)
- d = 1190Å (1.7% decrease)
- V_p = 53.84V (145% increase)

The performance of the resonator tank before and after optimization is shown in Figure 6(a). The resonant frequency is shifted from 31.07MHz to 30.04MHz. Phase noise of the oscillator is reduced from 120dBc/Hz to 129dBc/Hz at 1 kHz (see Figure 6(b)). Q factor is enhanced by 19%. Also, insertion loss is reduced from 17.15dB to 0.15dB.

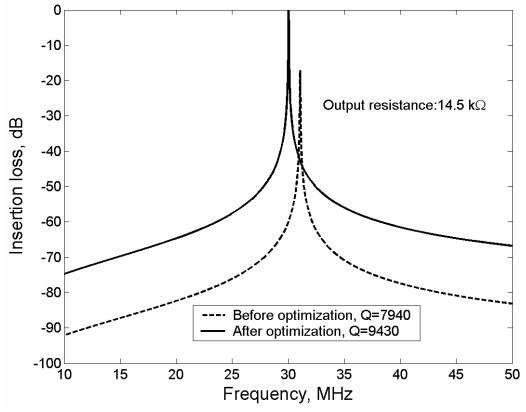

(a)

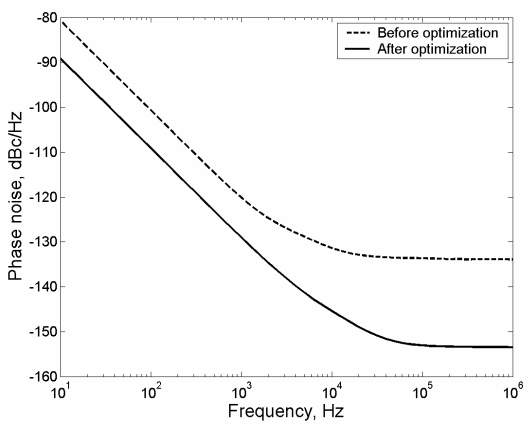

(b)

Figure 6: Circuit responses before and after optimization; (a) Insertion loss for the resonator tank. (b) Harmonic balance simulation results for phase noise.

To demonstrate the accuracy of the developed ANN model, the optimized values are used as input for the FEM simulation and its response is compared with that obtained by the circuit simulator. As seen in Figure 7, good agreement between the FEM and ANN model is observed.

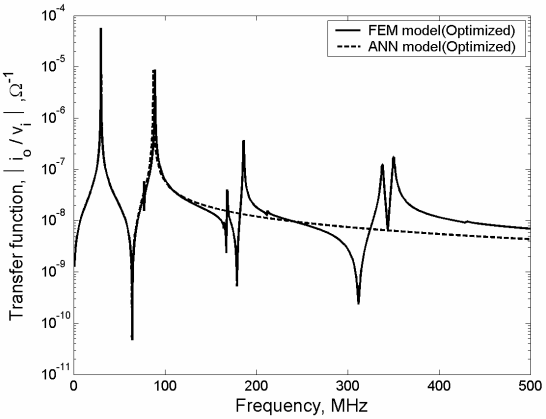

Figure 7: Comparison between the ANN and FE models upon inserting optimized values.

The relative error for the resonant frequency remains 0.40% (ANN: 30.04MHz and FEM: 29.91MHz). Note that the dataset obtained during optimization was not included in the training set. A significant reduction in simulation time is also observed. For a single run, 2.8secs and 93secs are measured for the ANN model (in the circuit simulator) and the FEM model, respectively.

CONCLUSIONS

This paper demonstrated an efficient modeling approach for the design of RF ICs with embedded MEMS devices and related components. Large savings in computational time and memory is achieved while the full-wave accuracy is retained. Proposed methodology is applicable for design and optimization of RF circuits and systems containing any class of MEMS devices.

REFERENCES

[1] K.J. Winchester and J.M. Dell., *Conf. Optoelectronic and Microelectronic Materials and Devices,* pp.324 – 327, 2000.

[2] D. Li and Y. Zhang, *Int. Conf. MEMS, NANO and Smart Sys.*, pp.292–296, 2003.

[3] *Z.* Wang, B. Jensen, J. Volakis, K. Saitou, K. and Kurabayashi., *IEEE APS Int. Symp.*, Vol. 2, pp.173–176, 2003.

[4] N. Bushyager, K. Lange, M. Tentzeris, and J. Papapolymerou, *IEEE MTT-S,* Vol. 2, pp.883–886, 2002.

[5] R. Marcelli, *et al.*, *Electronics Letters,* Vol. 40, pp.1272–1274, 2004.

[6] P.V. Nikitin, *et al*. *Proc. 5th Int. Symp. Quality Electronic Design*, pp.244–249, 2004.

[7] L.D. Gabbay and S.D. Senturia., *J. Microelectromech. Syst*., Vol.9, pp.262–269, 2000.

[8] Y.J. Lee *et al*., *Int. J. RF and Microwave Computer Aided Eng.*, Vol.14, pp. 302–316, 2004.

[9] K. Wang, A.-C. Wong, and C.T.-C. Nguyen., *J. Microelectromech. Syst*., Vol. 9, pp.347–360, 2000.

[10] Y.H. Park and K.C. Park., *J. Microelectromech. Syst*., Vol.13, pp.238–247, 2004.

[11] Advanced Design System, Ver. 2003A, *Agilent, Inc*., http://eesof.tm.agilent.com

[12] Maia, N.M.M., *et al*. 'Theoretical and experimental modal analysis', (*Research Studies Press Ltd*., 1997), Ch.1.

[13] Q.J. Zhang and K.C. Gupta, 'Neural networks for RF and microwave design', (*Artech House*, 2000), Ch. 4.

[14] D.C. Montgomery, 'Design and analysis of experiments', (*John Wiley & Sons, Inc.*, 1997), pp.339, 588.